# EXPERIMENTALLY OBSERVED NONLINEAR DISSIPATION LINKED TO CONTRIBUTIONS FROM GAS DAMPING AND TED IN MEMS FLEXURAL MODE RESONATORS

*Anne L. Alter[1], Gabrielle D. Vukasin[1], Ian B. Flader[2], Hyo Jin Kim[1], Yunhan Chen[3], Daniel D. Shin[1], and Thomas W. Kenny[2]*
[1]Stanford University, Stanford, California, USA
[2]Invensense Inc., San Jose, California USA
[3]Apple Inc., Cupertino, California, USA

## ABSTRACT

This paper presents an investigation into the origin of nonlinear dissipation in MEMS flexural mode resonators driven in a highly nonlinear regime. By comparing devices with different combinations of thermoelastic and gas damping, and utilizing the ringdown response at different pressures, we observe a larger presence of nonlinear dissipation in pressure damped resonators, but also continue to observe some nonlinear dissipation at high vacuum suggesting additional nonlinear contributions from thermoelastic dissipation.

## KEYWORDS

Nonlinear Dissipation, Nonlinearity, Damping, Thermoelastic Dissipation, Gas Damping

## INTRODUCTION

### Background

As sensor size gets smaller, driving MEMS resonators at large amplitudes in a nonlinear regime is necessary to achieve a suitable signal-to-noise ratio. Therefore, nonlinear operation of MEMS devices is becoming more commonplace with research focusing on the potential benefits of nonlinear operation or compensation schemes needed to make up for the nonlinear effects. However, despite this research, an overlooked phenomenon in nonlinear resonators is nonlinear dissipation, which is dissipation dependent on vibrational amplitude. This could have impacts for devices like gyroscopes, accelerometers, and even tuning forks driven at large amplitudes.

The quality factor, Q, a metric used to describe the dissipation in an oscillator, is extremely important in MEMS resonators as it is directly linked to the performance and reliability of these devices. The dissipation force in resonators has typically been calculated by linearly relating a single coefficient with the device velocity ($b_1\dot{x}$), and this assumption has been made for resonators at the macro scale down to the nanoscale. However, as devices are scaled down in size and driven in a highly nonlinear dynamic range, there have been observations of damping that cannot be described by this single damping coefficient and thus are nonlinear in nature.

Researchers have observed nonlinear dissipation at the nanoscale in doubly clamped beams made of carbon and graphene [1], $Pd_{0.15}Au_{0.85}$ [2], and in magnetomotively driven diamond resonators [3]. Furthermore, nonlinear dissipation has been observed at the microscale in a MEMS single crystal silicon DA-DETF using the ringdown response to quantify the magnitude of the nonlinear dissipation coefficients [4]. Nonlinear dissipation has also been observed other materials at the macro-scale. One study was performed on macro-scale cantilever beams made of aluminum, and linked the nonlinear dissipation to contributions of gas damping and thermoelastic dissipation (TED) [6], which is similar to the study in this paper.

Despite some of the recent experimental developments in micro and nanoscale nonlinear dissipation, there has been little theoretical work performed. One theoretical study in MEMS did link nonlinear dissipation to thermoelastic dissipation through simulations of MEMS cantilevers [5] and another used Euler-Bernoulli bending, but was unable to capture the full magnitude of the nonlinear dissipation [2].

So far though, none of the research has been able to make specific conclusions about the exact origin of the nonlinear dissipation. The studies have most commonly speculated that nonlinear dissipation is due to clamping losses (phonon tunneling) [1, 3], nonlinearities in phonon-phonon interactions [1, 4], and geometric nonlinearities modifying the shape and stiffness of the structures [1, 2, 3, 5].

This work is the first to experimentally investigate the origin of nonlinear dissipation for MEMS flexural mode resonators fabricated in an ultraclean environment with different combinations of thermoelastic and gas damping. We perform ringdown experiments at the device encapsulation pressure and at ultra-high vacuum to try isolate the effects of the different sources of damping and make conclusions about the origins. This study can help the field to better understand how we can begin to isolate some of these damping factors and, in general, what metrics could be important when designing MEMS resonators, particularly those driven in a highly nonlinear regime.

## EXPERIMENT METHODS

### Device Design

The in-plane modes of central-anchored wheel (64 kHz) and double-anchored beam (102 kHz) flexural resonators are studied. As shown in Figure 1, a FEM model was created and the simulated quality factor due to thermoelastic dissipation in the wheel was determined to be 163k, and in the DA-beam is 203k.

The experimentally measured quality factor of the wheel is 5k below the simulated value, and therefore this close match suggests that the primary damping mechanism is likely due to thermoelastic dissipation. In addition, the DA-beam had a bigger discrepancy with the measured value, about 81k below the simulated value, suggesting the presence of another damping mechanism.

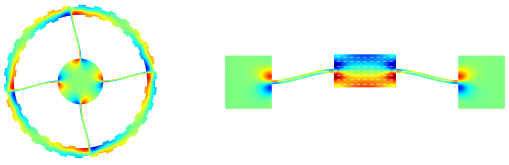

$Q_{TED}$ = 163k
$Q_{measured}$ = 158k

$Q_{TED}$ = 203k
$Q_{measured}$ = 122k

*Figure 1: TED simulations of wheel and beam resonators.*

## Device Fabrication

The devices studied were fabricated with a 20um single crystal silicon (SCS) device layer in an ultra-clean, vacuum encapsulated package [7]. The fabrication process allowed for large transduction gaps (up to 50 um), which enable these devices to be driven at large amplitudes in a highly nonlinear regime.

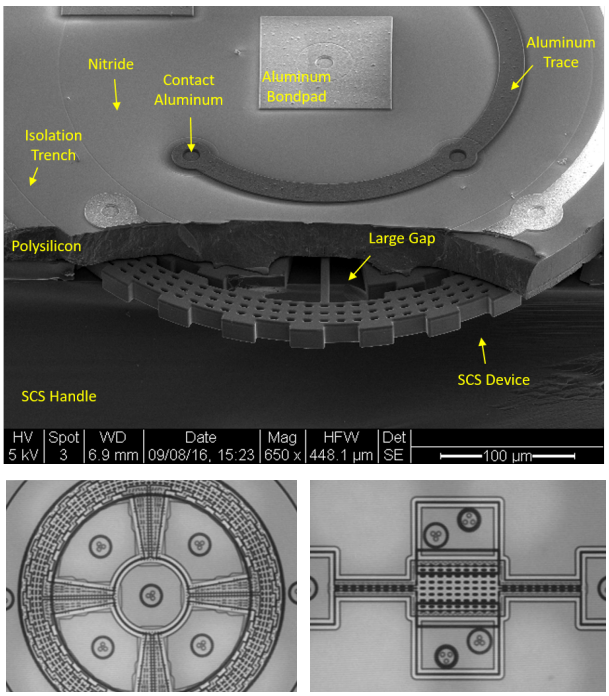


*Figure 2: SEM (top) and IR images (bottom) of the fabricated resonators*

As shown in Figure 2, the SEM image highlights the SCS device layer, the visible large gap in the wheel resonator, and the polysilicon encapsulation layer, which keeps the device sealed in an ultraclean environment. The IR images show a top view of the fabricated devices, with visible electrical contacts and large gaps.

## Mathematical Model

The devices in this study were driven at large amplitudes in a highly nonlinear regime, which can be characterized as a spring mass damper system with the Duffing equation shown in Equation 1 [8]. In Equation 1, $m$ is mass, $b_1$ is the linear dissipation coefficient, $k_1$ is the linear spring force, $k_3$ is the nonlinear Duffing parameter, $F$ is the force, $w$ is angular frequency, $t$ is time, and $x$ is displacement.

$$m\ddot{x} + b_1\dot{x} + k_1x + k_3x^3 = Fcos(wt) \quad (1)$$

To consider the potential effects of nonlinear dissipation, an additional dissipation term, $b_2$, which describes the effects of nonlinear dissipation at large displacements, is added to the equation, as shown in Equation 2 [8].

$$m\ddot{x} + (b_1 + b_2x^2)\dot{x} + k_1x + k_3x^3 = Fcos(wt) \quad (2)$$

## Experiment Methods

The devices were forced into highly nonlinear oscillation and driven into closed-loop resonance using a phase lock loop at the bifurcation point, which has been shown to be a stable operating point using closed-loop measurements [9]. The ringdown response was measured and repeated for a constant 35V bias voltage at a range of amplitudes. Short time Fourier transform methods were used to extract the amplitude, frequency, and quality factor associated with brief segments of the ringdown response, allowing for the extraction of these parameters as a function of amplitude.

In addition, the encapsulated parts were vented using a focused ion beam to drill an 8um x 8um hole into the cap layer (see inset of Figure 4). Venting the devices enabled them to be pumped down in a pressure chamber to pressures even lower than the encapsulation pressure. The ringdowns at high amplitudes were repeated at these low pressures and compared with those done at encapsulation pressure to determine if the amplitude dependence of the nonlinear dissipation had changed.

# RESULTS

## Responsivity

Open loop frequency-amplitude measurements, shown in Figure 3, show geometric hardening nonlinearities in both devices.

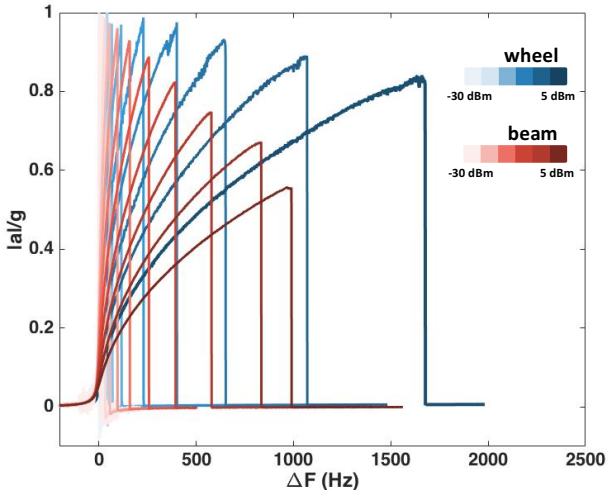


*Figure 3: Responsivity of wheel and DA-beam resonator showing a decrease in output (|a|) normalized by input signal (g), which suggests the presence of nonlinear dissipation.*

The output amplitude, which is normalized by the drive amplitude, is approximately 1 when the devices are

driven at low drive amplitudes. However, when driven at large amplitudes this normalized amplitude response decreases in both geometries, suggesting the presence of nonlinear dissipation. As shown in Figure 3, the beam resonator shows a much greater decrease in responsivity than the wheel resonator, suggesting a greater presence of nonlinear dissipation.

**Pressure Sweeps**

To determine the encapsulation pressure of the devices, pressure sweeps, shown in Figure 4, were performed after venting the parts. The inset of Figure 4 shows the venting hole that was created in the polysilicon cap using a focused ion beam. The venting hole penetrates through the cap layer and is placed over a trench that is connected to the device layer, but located away from the device itself. This allows the device layer to be exposed to atmospheric pressure through the trench channel without damaging the device itself.

The quality factor before venting the encapsulated parts was compared to the pressure sweep to determine the encapsulation pressure. From the sweep, it is determined that the encapsulation pressure is approximately 5e-1 Pa. Venting the devices and pumping them down to low pressures also enabled the study of the effects of gas damping on quality factor, which will be discussed in the next section.

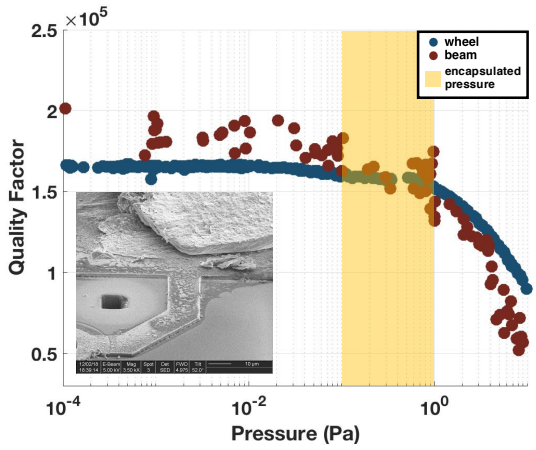


*Figure 4: Pressures sweeps of the two devices; inset shows hole created with focused ion beam to vent the device through the encapsulation layer to atmospheric pressure.*

**Quality Factor and Amplitude**

The quality factor was measured for different segments of the ringdown response at both encapsulation pressure and at high vacuum in the vented parts. When the ringdown response is linear, such as in regions where the devices are driven at small amplitudes, the quality factor is constant through time and amplitude. However, in both resonator designs, when the ringdown is initiated from the device driven at a large amplitude, the quality factor is no longer constant over time and amplitude, with it decreasing at larger amplitudes.

As shown in Figure 5, the ringdown response of the wheel at high vacuum is slightly higher than at encapsulated pressure. At encapsulation pressure, the quality factor of the wheel in the linear regime is 161k. At high amplitudes, the quality factor bends to 148k. At high vacuum, the quality factor starts at a slightly higher value of 169k in the linear regime and bends to 156k in the nonlinear regime. The percent change in the quality factor between high and low amplitudes is -8% at encapsulation pressure and -7.7% at high vacuum.

As shown in Figure 6, the ringdown response of the DA-beam has a more significant difference between high vacuum and encapsualted Q, than the wheel. Overall, at encapsulation pressure, the quality factor in the linear regime is 122k and bends to 98k at high amplitude. At high vacuum, the quality factor starts at 173k and bends to 156k in the nonlinear regime. The percent change in quality factor between high and low amplitudes is -20% at encapsulation pressure and -9.8% at high vacuum.

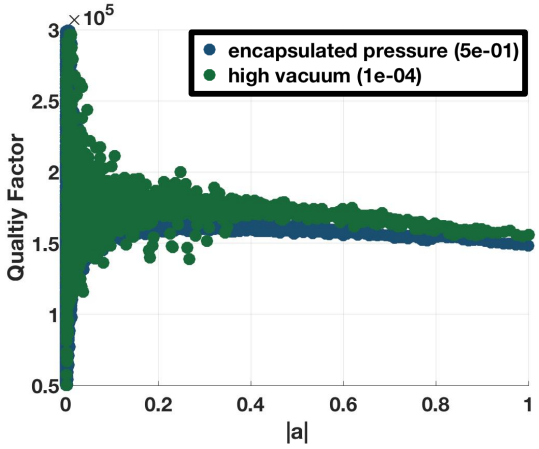


*Figure 5: quality factor vs. amplitude for wheel resonator derived from ringdowns when encapsulated and when vented and pumped down to high vacuum.*

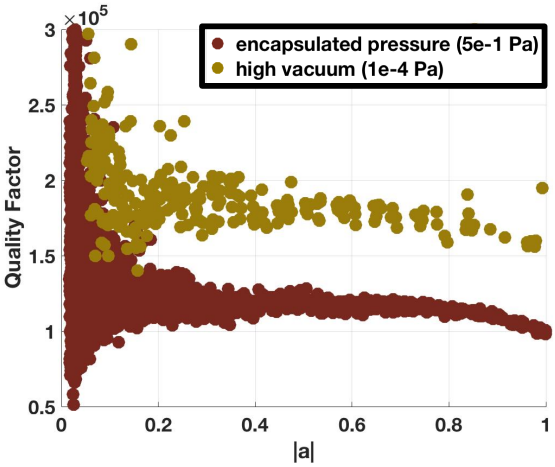


*Figure 6: quality factor vs. amplitude for beam resonator derived from ringdowns when encapsulated and when vented and pumped down to high vacuum.*

The Q-Amplitude plots are important in understanding the contribution of pressure damping to nonlinear dissipation. From the observed jump in quality factor at high vacuum in the DA-beam, we find that there is a

significant amount of pressure damping in this resonator, especially when compared with the wheel. We also observe that the percent change in the amplitude dependence of the quality factor changes more significantly between encapsulated and high vacuum for the DA-beam than for the wheel. Furthermore, these plots show that we continue to see nonlinear dissipation at high vacuum in both devices, suggesting that there are nonlinear contributions from TED.

## CONCLUSIONS

From these results, we can see that both the beam and wheel resonators have dissipation that can be attributed to both TED and gas damping. From the pressure sweeps, we can conclude that the beam resonator has more gas damping than the wheel resonator due to the larger decrease in quality factor between encapsulation pressure and high vacuum. From the simulations, we can reasonably conclude that the primary damping mechanism in the wheel resonator is TED. The beam resonator did not match the TED simulation as closely, even at low vacuum, so it is possible that there is another damping mechanism that contributes to the losses, such as anchor damping, or that the device got damaged during the FIB process.

Overall, these results show that the contributions from nonlinear dissipation are more significant in pressure limited resonators, but there is still some significant nonlinear dissipation present at high vacuum, which is likely linked to amplitude-dependent dynamic properties (frequency, stiffness, elasticity) contributing to changes in TED. These results closely align with the study done on macro-scale aluminum cantilever beams, which concluded that gas damping proportional to velocity squared dominates at large amplitudes and dissipation proportional to velocity dominates at low amplitudes [6].

In addition to showing that nonlinear dissipation can be a significant factor in MEMS resonators driven in a nonlinear regime, we conclude that there are important contributions from both gas damping and TED, with the contributions in pressure limited resonators being more significant.

## ACKNOWLEDGEMENTS

This work was supported by the Defense Advanced Research Projects Agency (DARPA) grant "Precise Robust Inertial Guidance for Munitions (PRIGM)", managed by Dr. Ron Polcawich, Contract Number #N66001-16-1-4023. This work was performed in part at the Stanford Nanofabrication Facility (SNF), supported by the National Science Foundation under Grant ECS-9731293. Special thanks to all the staff at SNF for their help during the fabrication process.

## REFERENCES

[1] E. Eichler, et al., "Nonlinear Damping in Mechanical Resonators Made from Carbon Nanotubes and Graphene", *Nature Nanotechnology*, vol. 6, no. 6, pp. 339-342, 2011.

[2] S. Zaitsev, et al., "Nonlinear Damping in Micromechanical Oscillator", *Nonlinear Dynamics*, vol. 67, no.1, pp. 859-883, 2012.

[3] M. Imboden, et al., "Nonlinear Dissipation in Diamond Nanoelectromechanical Resonators", *Applied Physics Letters*, vol. 102, no. 10, pp. 103502, 2013.

[4] P.M. Polunin, et al., "Characterization of MEMS Resonator Nonlinearities Using the Ringdown Response", *J. Microelectromech. Syst.*, vol. 25 no. 2, pp. 297-303, 2016.

[5] C. Méndez, et al., "Effect of Geometrical Nonlinearity on MEMS Thermoelastic Damping", *Nonlinear Analysis: Real World Applications*, vol. 10, no. 3, pp. 1579-1588, 2009.

[6] Baker, et al., "Air and internal damping of thin cantilever beams", *International Journal of Mechanical Sciences*, vol. 9, no. 11, pp. 743-766, 1967.

[7] Y. Chen, et al., "Robust Method of Fabricating Epitaxially Encapsulated MEMS Devices with Large Gaps", Journal of Microelectromechanical Systems, 26, 6, (2017).

[8] R. Lifshitz, et al., "Nonlinear dynamics of nanomechanical and micromechanical resonators." *Review of nonlinear dynamics and complexity*, vol. 1, pp. 1-52, 2008.

[9] H. K. Lee, et al., "Stable operation of MEMS oscillators far above the critical vibration amplitude in the nonlinear regime," *J. Microelectromech. Syst.*, vol. 20, no. 6, pp. 1228–1230, 2011.

## CONTACT

*A.L. Alter, tel: +1-651-808-3803; annealtr@stanford.edu